Pharm Res (2014) 31:3211–3224
DOI 10.1007/s11095-014-1413-4

RESEARCH PAPER

Dissolution Testing of Powders for Inhalation: Influence of Particle Deposition and Modeling of Dissolution Profiles

Sabine May • Birte Jensen • Claudius Weiler • Markus Wolkenhauer • Marc Schneider • Claus-Michael Lehr

Received: 31 January 2014 / Accepted: 6 May 2014 / Published online: 23 May 2014

ABSTRACT

Purpose The aim of this study was to investigate influencing factors on the dissolution test for powders for pulmonary delivery with USP apparatus 2 (paddle apparatus).

Methods We investigated the influence of dose collection method, membrane holder type and the presence of surfactants on the dissolution process. Furthermore, we modeled the *in vitro* dissolution process to identify influencing factors on the dissolution process of inhaled formulations based on the Nernst-Brunner equation.

Results A homogenous distribution of the powder was required to eliminate mass dependent dissolution profiles. This was also found by modeling the dissolution process under ideal conditions. Additionally, it could be shown that influence on the diffusion pathway depends on the solubility of the substance.

Conclusion We demonstrated that the use of 0.02% DPPC in the dissolution media results in the most discriminating and reproducible dissolution profiles.

In the model section we demonstrated that the dissolution process depends strongly on saturation solubility and particle size. Under defined assumptions we were able show that the model is predicting the experimental dissolution profiles.

KEY WORDS aerodynamic diameter (MMAD) · Andersen cascade impactor · Nernst Brunner equation · paddle apparatus

ABBREVIATIONS

aACI	Abbreviated Andersen cascade impactor
ACI	Andersen cascade impactor
ACN	Acetonitrile
API	Active pharmaceutical ingredient
DPPC	Dipalmytoylphosphatidylcholine
EMA	European Medicines Agency
FDA	Food and Drug Administration
FPD	Fine particle dose
HPLC	High performance liquid chromatography
mACI	Abbreviated Andersen cascade impactor with stage extension and modified filter stage
PBS	Phosphate buffered saline
RC	Regenerated cellulose membrane
RP	Reversed phase
SDS	Sodium dodecyl sulfate
SE	Stage extension
SEM	Scanning electron microscopy
USP	United States Pharmacopoeia

LIST OF SYMBOLS

ρ	Density
η_{water}	Dynamic viscosity of water at 37°C
c_s	Solubility of drug
c_t	Concentration of the drug in the solution at time t
D	Diffusion coefficient of substance in the solvent
d_{aero}	Aerodynamic particle diameter
d_{geo}	Geometric particle diameter

Electronic supplementary material The online version of this article (doi:10.1007/s11095-014-1413-4) contains supplementary material, which is available to authorized users.

S. May · M. Schneider · C.-M. Lehr
PharmBioTec GmbH, Saarbrücken, Germany

S. May · B. Jensen · C. Weiler · M. Wolkenhauer
Boehringer Ingelheim Pharma GmbH & Co KG, Ingelheim, Germany

M. Schneider
Pharmaceutics and Biopharmacy, Philipps-Universität Marburg, Marburg Germany

C.-M. Lehr (✉)
Biopharmaceutics and Pharmaceutical Technology, Saarland University Saarbrücken, Germany
e-mail: lehr@mx.uni-saarland.de

C.-M. Lehr
Helmholtz Institute for Pharmaceutical Sciences Saarland, Helmholtz Center for Infection Research, Saarbrücken, Germany

dm	Mass of solid material at time t
dt	Time interval
f_1	Difference factor
f_2	Similarity factor
h	Diffusion (boundary) layer thickness
k	Shape factor
m	Amount of drug released
N_e	Number of particles in a particle size fraction
r	Radius
R_t	Mean percent drug released at each time point for reference product
S	The surface area of the particles
S_e	The surface area of each particle size fraction
t	Time
T_t	Mean percent drug released at each time point for test product
V	Volume
V_M	Van der Waals volume
X_e (0)	The amount of undissolved drug in a particle size group
X_e(t)	The amount of undissolved drug in a particle size group e
X_{sum}(t)	Total amount of undissolved drug at time t

INTRODUCTION

Dissolution testing for drug release control of active pharmaceutical ingredients (API) using USP apparatus 2 (paddle apparatus) is a well-established method (1–3) for oral semi solid and solid dosage forms or transdermal systems. Dissolution testing of respirable powders is not necessary due to the use of substances with good solubility and thus quality control testing focused on aerodynamic particle size distribution of API and excipients (1,4).

Even for inhaled drugs, the recent development of new pharmaceutical molecules has tended to generate mostly poorly soluble substances (5). Consequently, particles need a longer time to dissolve which might cause problems for bioavailability due to the interfering time scales of dissolution and clearance mechanisms.

Therefore, in the future dissolution testing is likely to deserve increasing consideration in the development of inhalation powders (1,6). So far different dissolution techniques for powders for inhalation such as Franz Diffusion Cell (7–9), a Transwell® system (10), the paddle apparatus with membrane holder (7,11), and a flow through cell (7,8,12) have been described in literature. These techniques used as dissolution media buffers (pH 6.8–7.4) *e.g.* phosphate buffered saline (PBS) (7,8,10) or simulated lung fluid (13) with or without surfactant were used. The surfactants used were dipalmytoylphosphatidylcholine (DPPC), Tween® 80 (11), and SDS (14). Tween® 80 and SDS are both exogenous surfactants. In contrast, DPPC is a physiological compound, contributing to approximately 40% of the natural lung surfactant (15).

From the beginning efforts were taken to theoretically describe and predict the effects of experimental dissolution testing (16). A high percentage of the model approaches rely on the hypothesis that the dissolution process is divided into two steps (17): first, the dissolution of the solid to form a stagnant film or diffusion layer, and second, the diffusion of the solute from this layer to the bulk liquid (16,18). Different mathematical expressions for describing this dissolution process were obtained by Noyes, Whitney, Brunner, Tolloczko, Nernst, Brunner, Hixson, and Crowell. These models were applied specifically to oral dosage forms or in the case of Higuchi ointments (16). In the literature for dissolution testing of powders for inhalation the dissolution profiles were fitted with models describing the kinetic of the process (7,8,19,20).

We previously compared several dissolution techniques (7). We were able to demonstrate that the classic paddle apparatus modified with a specially designed holder for the sample bearing membrane ("membrane holder") was the most suitable and also best discriminating technique. But several questions still remained unanswered, especially concerning critical factors with impact on the dissolution process. In this follow up study we focus on these impact factors not only from an experimental but also from a theoretical point of view. In the first, experimental part of this study we investigated the influence of dose collection method, membrane holder design and choice of surfactants on the dissolution profile. In the second, theoretical part, we simulated dissolution profiles based on the Nernst—Brunner equation. The modeling served two purposes: 1) to explore the effect of varying the particle mass on the membrane, the effect of particle shape and size on the dissolution as well as the effect of the thickness of the diffusion layer and the solubility, and 2) to compare the model with experimental dissolution data from the first part of this paper.

PART I EXPERIMENTAL DATA

Material and Methods

Material

Substance A (for the free base: log D 2.4, molecular weight 683.8), an API currently in the research pipeline, was obtained from Boehringer Ingelheim (Ingelheim, Germany). Budesonide (Cipla, India), Substance A dibromide and Substance A crystalline base were micronized using jet

milling. Spray drying of Substance A base led to the amorphous form. The solubility data of the substances in phosphate buffered saline (PBS) buffer pH 7.4 (Sigma Aldrich Chemicals, Steinheim, Germany) and PBS buffer containing various surfactants are summarized in Table I (21).

KH_2PO_4 which was used as eluent buffer pH 3 and Acetonitrile (HPLC grade) were purchased from Merck (Darmstadt, Germany). The membrane (regenerated cellulose, 100 mm diameter, 0.45 μm pore size) was obtained from Whatman (Dassel, Germany). HPLC vials were obtained from Macherey Nagel (Düren, Germany) and Waters (Milford, USA).

A Milli Q® system (Millipore, Molsheim, France) was used to produce purified water.

The surfactants used were dipalmytoylphospahtidylcholine (DPPC) (Lipoid, Ludwigshafen, Germany), Tween® 20 (Acros Organics, Geel, Belgium) and sodium dodecyl sulfate (SDS) (Karl Roth, Karlsruhe, Germany). Table I displays the sizes of self-assembled objects (*e.g.* micelles) in buffer as determined by dynamic light scattering.

High Performance Liquid Chromatography (HPLC)

All quantification measurements of substances were performed by HPLC (Alliance system, Waters GmbH, Frankfurt, Germany) with reversed phase chromatography (LiChrosphor 60 RP select B, 60×4 mm column, MZ Analysentechnik, Mainz, Germany) and UV/Vis detection (detector operates at 240 nm for Budesonide and 225 nm for Substances A). The eluent consisted of a buffer pH 3 and Acetonitrile (Budesonide 60/40, Substance A 65/35) and a flow rate of 1.7 ml min^{-1} was applied.

The column temperature was set to 40°C. The volume of each sample injected was 10 μl.

For the used substances the limit of quantification was determined (data not shown). For all substances multilevel calibration with external standards was performed.

Solubility Measurements

Saturated solutions of the different forms of Substance A and budesonide were prepared by adding the API to 25 ml PBS buffer, either with no surfactant or containing 0.2% SDS, 0.2% Tween® 20, or 0.02% DPPC. The flasks were stored in an overhead shaker protected from light at 22°C with 50%RH in a climate cabinet. After 24 h the suspensions were filtered using Spartan filter (13/0.45 RC, Schleicher & Schüll, Dassel, Germany) and diluted. Concentrations were determined by HPLC. Due to limited availability of Substances A, solubility measurements were performed only once. Budesonide measurements were done in triplicate.

Dose Collection

For dose collection an abbreviated Andersen cascade impactor (aACI) and its modifications were used (21) (Fig. 1). Substances were filled into Polyethylene capsules and were aerosolized using a HandiHaler® at the standard USP airflow conditions (4 kPa pressure drop, 4 l volume) for the aACI. The same flow rate was used for experiments with the modified ACI. The fill weight of the capsules varied between 0.5 and 4 mg in depending on how much was needed to deposit a homogenous particle mass on the membrane. In order to obtain a homogenous particle distribution on the membrane, a cylindrical shaped stage extension (SE) with a height of 5.8 cm was inserted between stage 1 and the filter stage. The stage extension and the aACI both have the same volume. The suction time was adapted to 0.85 s, mainly to achieve particle sedimentation on the membrane instead of impaction but still ensure complete emptying of the capsule. After the pump stopped, the optimal waiting time for sedimentation was determined to be 5 min. In addition to the normal ACI filter stage a modified filter stage (mFS) consisting only of three small bars, was used to change the flow and deposition pattern (21). A regenerated cellulose membrane (pore size 0.45 μm) was used as the filter. In the following mACI refers to the combination of abbreviated ACI with stage extension and modified filter stage, for the arrangement of aACI with stage extension; aACI + SE is used.

Table I Solubility Data for Budesonide (mean ± SD) and Substances A in PBS Buffer With and Without Surfactant and the Sizes of Self-assembled Surfactant Objects/Micelles. The Hydrodynamic Diameter was Determined by Dynamic Light Scattering

	Solubility of budesonide	Substance A			Object size Ø [nm] (21)
		Dibromide	Amorphous base	Crystalline base	
PBS buffer	17 μg/ml (7) ± 0.2 μg/ml	265 μg/ml (7)	211 μg/ml (7)	7 μg/ml (7)	–
PBS buffer + 0.02% DPPC	21 μg/ml (21) ± 0.4 μg/ml	2,505 μg/ml	144 μg/ml	6 μg/ml	1,106
PBS buffer + 0.2% Tween® 20	40 μg/m (21) ± 0.3 μg/ml	3,865 μg/ml	663 μg/ml	22 μg/ml	7
PBS buffer + 0.2% SDS	406 μg/ml (21) ± 5.4 μg/ml	2,033 μg/ml	504 μg/ml	847 μg/ml	11

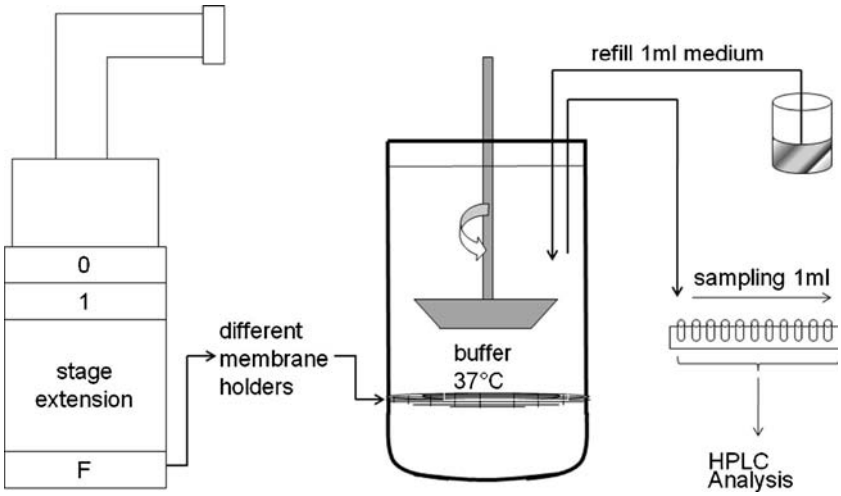

Fig. 1 Modified from (7): Andersen cascade impactor with stage extension and modified/ standard filter stage for dose collection (*left*). After dose collection the membrane is placed into the membrane holder or the membrane of the sandwich holder with fine particles towards the watch glass. Afterwards the membrane holder is placed into the paddle apparatus (*right*). The paddle apparatus is connected to a sampling and a refill unit. For detailed schematic of the filter holders please see Fig. 2.

Dissolution Tests

USP apparatus 2 (paddle apparatus, Sotax, Lörrach, Germany) with membrane holder was used as described for dissolution testing (7,11) (Fig. 1). The "standard" membrane holder (Copley Scientific, Nottingham, UK) consists of a watch glass and a plastic mesh to fix the membrane. Dissolution tests were performed with a stirring speed of 100 rpm at 37°C in PBS buffer pH 7.4. The sampling was automated according to a defined time schedule. To maintain a constant volume of dissolution medium, the solvent removed during sampling was refilled with fresh, pre-warmed dissolution medium. After dissolution testing, residual amounts of drug in and on the membrane and on the watch glass were determined by washing both parts with 50 ml solvent each (ACN for Budesonide and Substance A base, and buffer for Substance A dibromide). The total amount of drug initially loaded on the membranes was determined using the maximum of the cumulatively released amounts plus the remaining quantity on the membrane (determined at the end of each experiment). The fraction of released drug was calculated by dividing the amount of drug released by the initial drug mass loaded on the membrane (7).

The following experiments (under sink conditions) were performed to evaluate the:

a) best dose collection method

First, three different dose collection methods were compared (aACI, aACI + SE, mACI). Second, experiments determining the effect that different masses (FPD) on the membrane have on the dissolution process were evaluated. These experiments were only performed for Budesonide (21).

b) different types of dissolution membrane holders

The best method from a) was used as the dose collection method. For dissolution of Budesonide the following three membrane holders were tested.

- commercially available membrane holder from Copley (S1A) as described above
- blocked membrane holder (S1B)

  The blocked membrane holder is intended to prevent diffusion along the edge of the membrane. Onto the watch glass of the commercial available membrane holder the membrane is placed and locked at the rim with a stainless steel ring utilizing an o-ring.
- membrane sandwich holder (S1C)

  This membrane holder consists of two stainless steel rings and a mesh. After dose collection, the membrane is covered with a second empty membrane, and placed on the mesh. The mesh and the membranes are clamped in-between the two stainless steel rings.

c) dissolution medium with surfactant

Experiments were performed with the best dose collection method from a) and standard membrane holder. PBS buffer with and without 0.02% DPPC was used as dissolution medium. In addition, experiments with the blocking membrane holder and PBS buffer containing 0.02% DPPC were performed.

Data Treatment

Dissolution profiles were compared with fit factors as a statistical tool to decide if two profiles are similar or not. For getting a high statistical power the difference factor (f_1) (Eq. 1) and the similarity factor (f_2) (Eq. 2) of the Food and Drug Administration (FDA) and the European Medicines Agency

(EMA) require 12 individual values for each product (22,23). Due to a limited number of values ($n=3$) the statistical power of the test used is reduced.

Difference factor

$$f_1 = \frac{\sum_{t=1}^{n} |R_t - T_t|}{\sum_{t=1}^{n} R_t} \quad (1)$$

Similarity factor

$$f_2 = 50 * log\left[\frac{1}{\sqrt{1 + \frac{1}{n}\sum_{t=1}^{n}(R_t - T_t)^2}} * 100\right] \quad (2)$$

Where n is the number of dissolution sample time points, R_t and T_t are the mean percent of drug released at each time point for the reference and test product. Two curves are considered as similar when $f_2 > 50$ and for $f_1 < 15$ (22,23).

Results

Solubility Measurements

All substances were used in concentrations above their critical micelle concentration. The surfactants Tween® 20 and SDS in the concentration used increase the solubility of the substances under investigation. Depending on the substances, Tween® 20 increases the solubility 2–15 times and SDS 3.5–20 times. Only DPPC showed a high increase of the solubility of Substance A dibromide (10 times). No increase for the other substances could be shown.

Regarding micelle size and pore size of the regenerated cellulose membrane (0.45 µm), only Tween® 20 and SDS micelles are able to pass through the membrane. In contrast, the DPPC objects are too large for passing the cellulose membrane. Nevertheless, the surfactants might migrate through the membrane in non-assembled state.

Dissolution Tests

Impact of Dose Collection Method on the Dissolution Process. Figure 2 demonstrates the impact of dose collection method on the dissolution profile. The dissolution process is slower by using the aACI than by the use of mACI having the same particle mass ($D_{aero} < 5$ µm = fine particle dose (FPD)) on the filter. The SEM insets illustrate that the mACI yields a more homogenous particle distribution on the filter compared to the aACI where dark areas are visible. These areas are in line with the holes of the filter stage and contain a high number of agglomerated particles (data not shown). For this set up aACI + SE the dissolution profile is similar regarding the respective test to the one with modified filter stage (mACI) (table S1). The amount of FPD on membrane is increased (approximately 1 mg) to highlight the effect of the dose collection method on the SEM pictures.

Therefore, the holes of the filter stage that were visible with the aACI setup are also visible with the aACI + SE set up. Nevertheless, the shape of the holes is not as clearly defined as in the aACI SEM pictures.

Impact of Particle Mass on the Dissolution Process. The impact of particle mass on the dissolution process is shown in Fig. 3. The higher the mass of particles on the membrane, the slower the dissolution is. Although mass differences (200 µg) for the aACI are the same as compared to the mACI, the differences in dissolution profiles for the aACI are much larger than for the mACI. Fit factors ($f_1 = 9.4$; $f_2 = 59.1$ (table S1)) confirm the similarity of the mACI dissolution profiles obtained with different masses on the membrane. The fit factors show no similarity for the aACI profiles ($f_1 = 34.9$; $f_2 = 30.8$ (table S1)).

Comparison of Different Membrane Holder Types. Figure 4 shows no significant difference between the different membrane holder setups and the fit factors (table S1) indicate similarity of the different dissolution curves.

Dissolution Medium Containing Surfactant. As expected due to the low solubility of Substance A crystalline base, it shows the slowest dissolution process, regardless of the dissolution medium or membrane holder (Fig. 5). In the following description of the results, Substance A crystalline base is not given any extra consideration, because the dissolution process is always slowest and varied not much. The expected rank order of dissolution profiles in buffer from the solubility results was Substance A dibromide, Substance A amorphous base, and Budesonide.

For pure buffer pH 7.4 as displayed in Fig. 5a the dissolution profiles of Substance A amorphous base, Substance A dibromide and Budesonide are similar especially in the first 20 min and discrimination between the substances is not possible. The fit factor test (table S1) supports these results. A comparison of the fit factors of the dissolution profiles of the dibromide and Budesonide is not definitive ($f_1 = 14.7$, $f_2 = 47.6$).

If PBS buffer with 0.02% DPPC is used as the dissolution medium, Substance A amorphous base shows the fastest dissolution process. In the first 15 min, Budesonide shows a faster dissolution compared to Substance A dibromide. Later, due to a steeply rising slope Substance A dibromide reaches 90% dissolved amount after 25 min. In contrast, Budesonide takes 100 min. As the fit factor tests shows discrimination between all tested substances is possible (Fig. 5b, table S1). Furthermore, for the tested substances except for

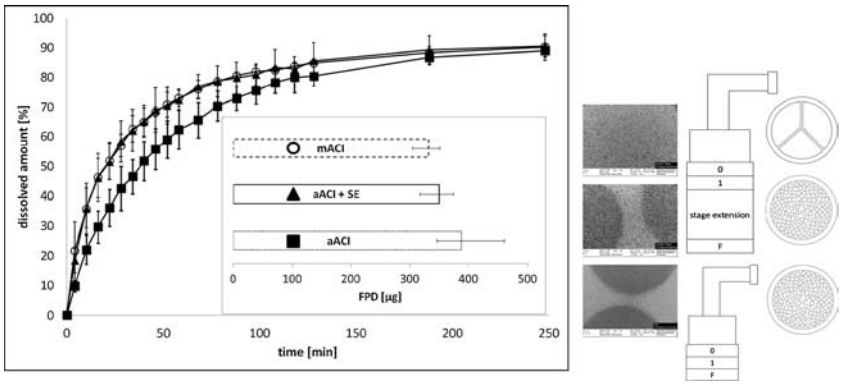

Fig. 2 Dissolution profiles by dose collection of Budesonide, with the mACI (*white circles*), aACI + SE (*black triangle*), and aACI (*black squares*); mean ± SD; $n=3$ with FPD on membrane; mean ± min/max; and SEM pictures (FPD on SEM picture membrane 1,000 µg) figure modified from (21).

the crystalline base the standard deviation of the dissolution profiles decreases with the use of 0.02% DPPC in the dissolution medium as compared to pure PBS buffer.

Surprisingly in Fig. 5c (PBS buffer pH 7.4 containing 0.02% DPPC, blocked membrane holder), Budesonide shows a faster rate of dissolution than Substances A dibromide and Substance A amorphous base. However, discrimination between the amorphous base and the dibromide is not possible ($f_1=6.4$, $f_2=65.1$, table S1). Compared to the set up without blocking (Fig. 5b) the dissolution of Substance A amorphous base and Substance A dibromide is decreased. Ninety percent dissolution is reached after more than 120 min.

PART II MODELING OF DISSOLUTION PROFILES

Theoretical Considerations

As described in the introduction there are several ways to model dissolution profiles. In this study an equation based on a diffusion layer concept was chosen. The so-called Nernst-Brunner equation, a modification of the Noyes-Whitney equation, combines the diffusion layer concept with Fick's second law (16).

In order to describe dissolution kinetics of monodisperse powders with the Nernst-Brunner equation several assumptions were made, *e.g.*, the surface area of particles change during dissolution, the dissolution of all particles contributes to the total concentration of the solution, and the thickness of the diffusion layer depends on the particle size (24). For the model, the form of the Nernst-Brunner equation shown below was used (Eq. 3). Where m is the mass of solid material at time t, S is the surface area of the particles, D the diffusion coefficient of the substance in the solvent, h is the diffusion boundary layer thickness, c_s is the saturation solubility of drug and c_t is the concentration of the drug in the solution at time t.

$$\frac{dm}{dt}=\frac{DS}{h}(c_s-c_t) \tag{3}$$

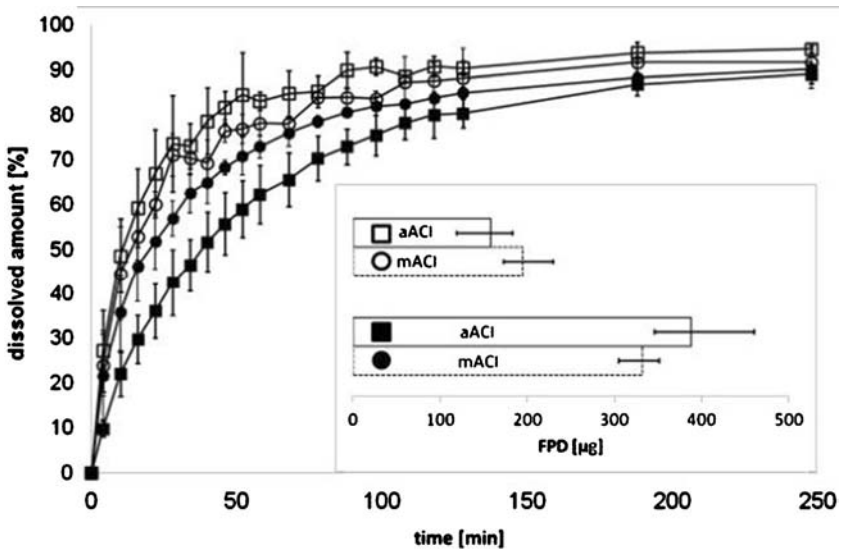

Fig. 3 Dissolution profiles of Budesonide for different deposited mass 200 µg of FPD on membrane (*open symbols*), 400 µg of FPD on membrane (*black symbols*), mACI (*dot*), a ACI (*squares*); mean ± SD, $n=3$ with FPD on membrane; mean ± min/max figure modified from (21).

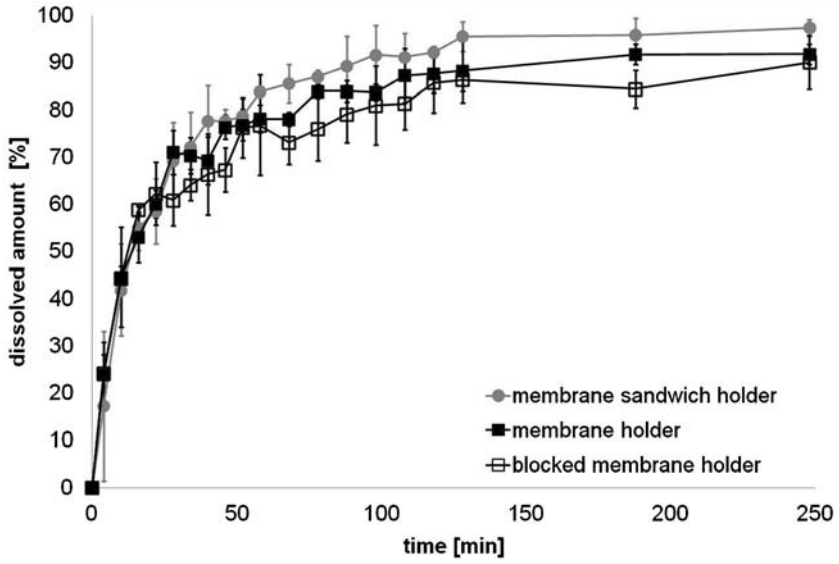

Fig. 4 Dissolution profiles of Budesonide for different membrane holders: membrane sandwich (*grey dots*), standard membrane holder (*black squares*), blocked membrane holder (*white squares with black border*); mean ± SD, $n = 3$.

The diffusion coefficient D was calculated by applying the Hayduk-Laudie Eq. (4) (25,26)

$$D = \frac{13.26 * 10^{-5}}{\eta_{water}^{1.4} * V_M^{0.589}}. \quad (4)$$

Where D is the diffusion coefficient, η_{water} the dynamic viscosity of water at 37°C. The Van-der-Waals volume V_M for each substance was theoretically determined in a two-step procedure from the chemical structure of the molecule using CORINA v3.46 (Molecular Networks (http://www.molecular-networks.com/products/corina) and MOE v2011.10 (CCG (http://www.chemcomp.com/)).

The behavior of the dissolution layer thickness h during the dissolution process is a well described parameter in the literature. Classically the diffusion layer is defined as the unstirred liquid layer adhering to the solid surface (18). Bisrat and Nystrom suggest that the diffusion layer might be smaller for small particles than for large particles (27). Overall, there is no agreement about the behavior of the diffusion layer during the dissolution process. Some authors postulate a time independent diffusion layer with a constant diffusion layer during particle shrinking (24). Others propose a time dependent diffusion layer, assuming a shrinking diffusion layer during particle shrinking (28,29) (Fig. 6). In contrast to this, there is a consensus that below a critical particle size the diffusion layer of a spherical particle can be approximated by the particle radius (h(t) = r(t)) (24,26,30). The critical particle radius is assumed to be 30 µm (29).

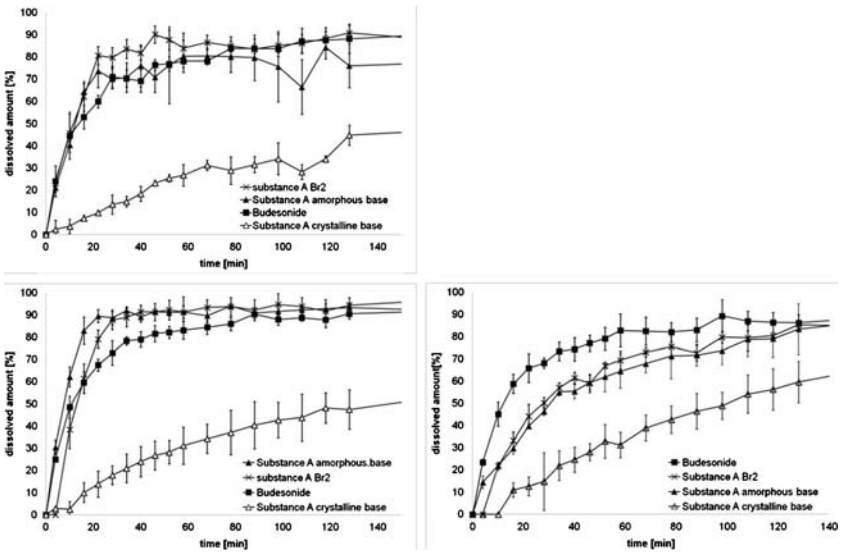

Fig. 5 Dissolution profile of Substance A Dibromide (*black x's*), Substance A amorphous base (*black triangles*), Budesonide (*black squares*) and Substance A crystalline (*open triangles*), mean ± SD, $n = 3$, (**a**) PBS buffer pH7.4. (**b**) PBS buffer containing 0.02% DPPC. (**c**) PBS buffer containing 0.02% DPPC, membrane holder with blocking.

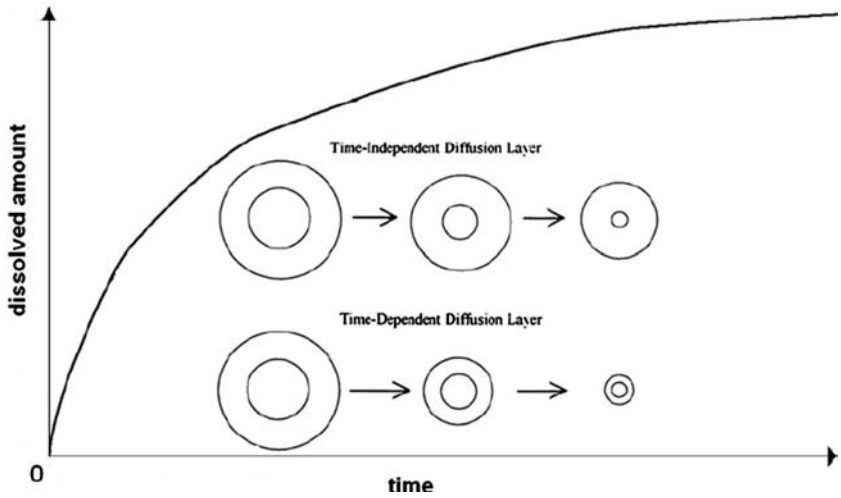

Fig. 6 Time dependence of diffusion layer, modified from (28).

Also discussed is the influence of the hydrodynamic conditions on the diffusion layer. Sheng *et al.* showed, that the paddle speed primarily influences the diffusion layer of large particles while particles with a particle radius smaller than 13 µm showed no impact on the diffusion layer (26).

Method

The modeling of the dissolution layer of particles in this paper is based on the following assumptions: sink conditions, spherical particles, well-stirred medium, isotropic dissolution, saturated solution at the surface of the particle/interface, constant diffusion coefficient along the diffusion layer and no impact of stirred medium on the dissolution due to the membrane. To guarantee sink conditions the API concentration in the medium should not exceed 10% of the saturation concentration (31). But the concentration changes that occur must be taken into account.

Because the particle size distribution from the experiments is polydisperse, the model takes into account different fractions according to the diameters resulting from the different ACI stages (32) (Table II).

In order to model the particle size distribution, a summation of monodisperse particle fractions is applied (29,33) (Eq. 5). Each group is represented by subscript e.

$$\frac{dX_{sum}(t)}{dt} = \sum_{e=1}^{n} \frac{dX_e(t)}{dt} = \sum_{e=1}^{n} \frac{DS_e(t)}{h_e t}\left(c_s - \frac{X_d}{V}\right) \quad (5)$$

$X_{sum}(t)$ is the total amount of undissolved drug at time t, $X_e(t)$ is the amount of undissolved drug in a particle size group e, S_e is the surface area of each particle size fraction, and h_e is the thickness of the diffusion layer, which depends on the particle radius r_e. The number of particles in each fraction is assumed to be time independent as described by Hintz *et al.* (29).

For spherical particles the surface area of a particle size group is calculated as described in the Eqs. 6–8 adapted from Hintz *et al.* and Okazaki *et al.* (29,33).

Equation 6 calculates the numbers of particles in each size group. This number stays constant over the whole dissolution process, except when $S=0$, then every particle is dissolved. With Eq. 7 the radius at time t is calculated. By combining Eqs. 6 and 7, it is possible to calculate the surface area of each particle size group that is presented for dissolution (Eq. 8).

$$N_e = X_e(0)\left(\frac{4\pi r_e(0)^3}{3}\rho\right)^{-1} \quad (6)$$

$$r_e(t) = \left(\frac{3X_e(t)}{4\pi\rho N_e}\right)^{1/3} \quad (7)$$

$$S_e(t) = N_e 4\pi r_e(t)^2 \quad (8)$$

Table II summarizes the parameters used. The particle mass corresponds to the mass on the membrane obtained from experimental data. Since the shape of our experimental particles is not spherical, the influence of shape on the dissolution process needs to be determined. Consequently, the aerodynamic diameters need to be converted into geometric ones.

For this calculation (Eq. 9), shape is important and a shape factor must be used. The shape factor for spherical particle is 1 and for cubic particles 1.08 (34). The volume and surface calculation was adapted for cubic particles. The assumed particle density of Budesonide is 1.27 gcm^{-3} (35).

Table II Data for Model Calculation

	Budesonide	Substance A		
		Crystalline base	Amorphous base	Dibromide
Solubility [μg/ml] (7)	17	7	211	265
vdWaals volume (Å^3)	419	619		701
Drug diffusion coefficient [cm^2/min]	6.19×10^{-6}	4.92×10^{-6}	4.92×10^{-6}	4.57×10^{-6}
Dissolution volume [ml]	1,000			
Diffusion layer thickness [μm]	h(t) = r(t)			
dt [min]	0.01			
Mass on membrane [μg]	200			
Particle size distribution [%] for fine particle fractions d_{aero} [μm] (7):				
5.29 μm	18.8%	10.4%	15.4%	14.2%
4.16 μm	29.7%	25.0%	25.7%	22.9%
2.49 μm	27.4%	37.2%	27.5%	52.1%
1.53 μm	18.1%	21.8%	21.9%	60.8%
0.7 μm	3.2%	3.7%	5.2%	8.2%
0.41 μm	1.3%	1.1%	2.5%	3.6%
0.21 μm	1.5%	1.1%	1.8%	1.1%

Particle sizes d_{aero} at time point $t=0$ are listed in Table II. The whole calculation is based on a stepwise procedure with $\Delta t=0.01$ min, until each particle fraction is dissolved.

$$d_{aero} = d_{geo}\sqrt{\frac{\rho}{k}} \tag{9}$$

The fine particle fraction on the membrane, the particle shape, the diffusion layer thickness, the solubility and the particle size distribution were varied for evaluating possible influencing factors for Budesonide. In each case the other parameters were kept constant.

Results

Influence of Particle Mass on the Membrane

For the theoretical model shown in Fig. 7a, the FPD on the membrane was varied (10, 100, 250, 500, 750, and 1,000 μg). The calculated dissolution curves show a minimal dependence on the mass deposited on the membrane. In the first 20 min the profiles are identical. As time is increasing the dissolution profiles diverge depending on the particle mass on the membrane, but only slightly. The fastest dissolution was shown for the smallest amount (10 μg) and the slowest was shown for the highest deposited mass (1,000 μg). Comparison of the profiles for 10 and 100 μg using the fit factor test shows similar almost identical profiles ($f_1=1.1$, $f_2=95.7$). The model is based on the assumption that there are no agglomerates and no dissolution interaction between the particles. Therefore, the model is not sensitive to different masses, and this result in similar dissolution profiles.

Influence of Particle Shape

The aerodynamic particle diameter was converted to the geometric diameter with Eq. 9 using either the shape factor for spherical or cubic particles.

In Fig. 7b the dissolution profile based on spherical particles is a little bit faster than for the cubic particles. However, the two profiles do not differ much and are similar to each other ($f_1=4.1$, $f_2=79.7$).

Influence of Diffusion Layer Thickness

Figure 7c demonstrates the influence of the diffusion layer thickness h on the dissolution profiles. Models A and D are based on the assumption that the diffusion layer thickness is directly dependent on the radius of each particle size group. In model D the diffusion layer shrinks with the particle size; in model A the diffusion layer stays constant while the particle dissolves. Model B is based on the assumption that the diffusion layer thickness for all groups correlates with the radius of the largest particles; in model C it correlates with the smallest. Models A and D are similar at the beginning of the dissolution process they have the same starting diffusion layer thickness. For later time points the models diverge. In model A, the constant h results in a slower dissolution process, than for model D where h decreases with the particle size. The dissolution curves of the models B and C differ strongly from A and

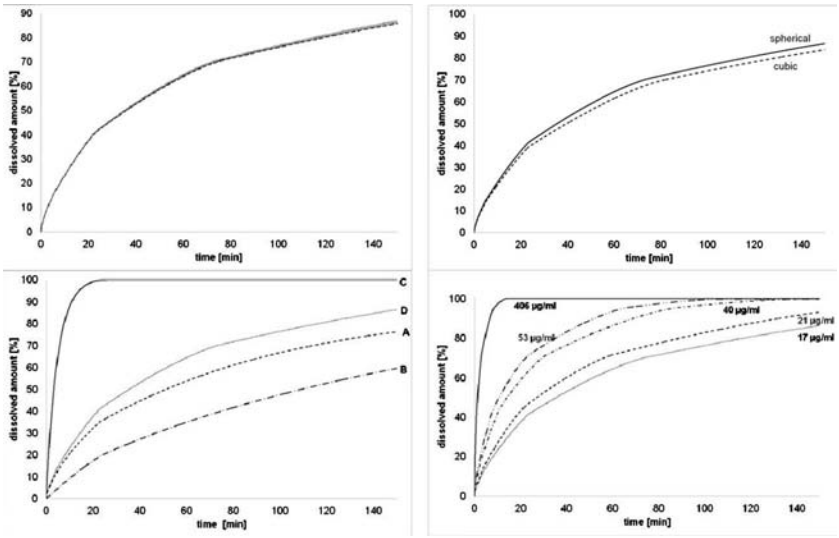

Fig. 7 Theoretical model for Budesonide with (**a**) A different mass on the membrane (10 μg dotted line, 100–750 μg *light grey to black*, 1,000 μg *dashed line*) (**b**) Spherical or cubic particles (**c**) Variations of diffusion layer thickness *h*. *A*: $h(0) = h(t) = d/2_{\text{every particle size fraction}} = \text{const.}$, h(0): 2.65×10^{-4} μm, 2.08×10^{-4} μm, 1.25×10^{-4} μm, 7.65×10^{-5} μm, 3.50×10^{-5} μm, 2.05×10^{-5} μm, 1.05×10^{-5} μm. *B*: $h(0) = h(t) = 2.65 \times 10^{-4} = \text{const.}$ *C*: $h(0) = h(t) = 1.05 \times 10^{-5} = \text{const.}$ *D*: $h(t) = d/2_{\text{every particle size fraction}}$ (t), see A for starting thickness, diffusion layer is shrinking with time. (**d**) Different solubility. The solubility data are based on the solubility measurement for Budesonide in PBS buffer pH 7.4 with different surfactants (Table I). The numbers on the curves indicate the respective saturation concentration.

D. B and C have a time independent diffusion layer, and for the different particle size classes the diffusion layer thickness is equal. It is obvious that a diffusion layer thickness that is too small results in a very fast dissolution profile and an *h* that is too large overall results in profile that is too slow.

Influence of Solubility

As expected, the dissolution profile is heavily dependent on the solubility of the substance in the dissolution medium (Fig. 7d). The higher the solubility, the faster the dissolution is.

Influence of Particle Size Distribution

In Fig. 8 the models for different particle sizes and particle size distributions on the membrane are compared with experimental data of Budesonide from Fig. 3. Table III summarizes the different particle sizes for the model. As expected, with a higher percentage of smaller particles, the dissolution results in faster dissolution profiles (b and a). The dissolution profiles of c and d are identical for the first 50 min, and later the profiles diverge. The model with the largest particles (c) has the slowest dissolution profile. As previously described, mACI shows a faster dissolution than aACI because of a more homogeneous distribution of particles on the membrane. When the modeled profiles are compared with the experimental data, the slower profile of aACI fits with the model a, c and d for the first 20 min. After approximately 50 min, model d no longer describes the experimental set up and model a fits best. Models a, c and d have a higher number of particles larger than 4.16 µm. In contrast; the dissolution profile of mACI fits with model b, which has a higher number of small particles and no similarity with model d.

Comparison of Experimental and Modeled Data for all Substances Used

Figure 9 compares experimental dissolution profiles with the associated model. For the model calculation, solubility of substances in PBS buffer containing 0.02% DPPC (Table I) and the data summarized in Table II were used and a time-dependent diffusion layer thickness was assumed. The model for Substance A amorphous base and Budesonide describe the experimental data quite well. The model for Substance A crystalline base is acceptable but the model for Substance A dibromide is differs significant from the experimental data.

Discussion

In the experimental section of this study we investigated the influence of different dose collection methods, membrane holders and surfactants on the dissolution process. In the second, theoretical section we incorporated these influencing factors into a model and tried to verify the theoretical considerations against experimentally observed dissolution profiles.

In our first study (7) we were able to demonstrate influence of particle mass (100 µg *vs.* 1,000 µg) on the membrane on the dissolution process and therefore on the dissolution profile.

In the experimental part of this study, we showed that changing the dose collection method reduces the influence

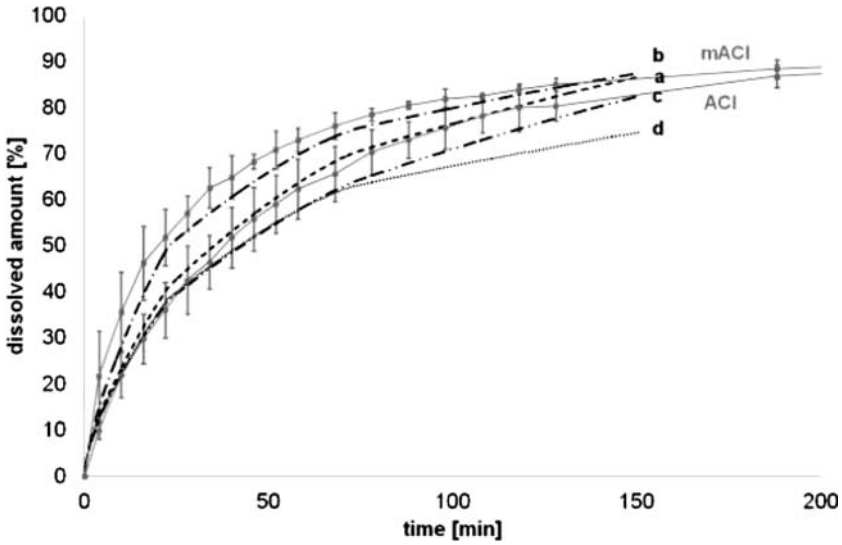

Fig. 8 Comparison of various modeled profiles for Budesonide with different particle size distributions on the membrane for *a–d* (see Table III) compared to experimental data, showing mACI: *square*; aACI: *dot*.

that the FPD has on the membrane on the dissolution. The SEM picture of the membrane after particle deposition with aACI reveals areas with a high number of agglomerated particles on the membrane, in line with the holes of the filter stage (36). Due to the occurrence of areas with a high particle load, even changes of less than 200 µg of mass on the membrane could be expected to strongly influence the dissolution process (Fig. 3). We were able to demonstrate that the use of a stage extension between filter stage and the first stage is necessary to reduce this effect. This filter stage in combination with the stage extension allows particle sedimentation instead of particle impaction. This result in a more homogenous almost single layer particle distribution, without agglomerates on the membrane . In consequence, the dependence of the dissolution process on mass is small. In the model section, under the assumption of optimum conditions—no agglomerates and therefore no dissolution interaction between the particle and its neighbors—we showed that FPD on the membrane has a negligible impact on the dissolution profile. Therefore, the optimal set up should reflect these conditions.

Table III Data for Fig. 8, a) Experimental Data, b) and c) Permutation of Percentages where b) has More Small Particles and c) Has More Large Particles, and d) Randomly Chosen Diameters for Assumption of Agglomerates

Particle diameter [μm]	a [%]	b [%]	c [%]	D	
				Diameter [μm]	[%]
5.29	18.8	18.8	29.7	8	18.8
4.16	29.7	18.1	27.4	5	29.7
2.49	27.4	27.4	18.8	2.49	27.4
1.53	18.1	29.7	18.1	1.53	18.1
0.7	3.2%				
0.41	1.3%				
0.21	1.5%				

The blocked membrane holder was used to reduce the effect of diffusion along the edge of the membrane instead of diffusion directly through the membrane. Interestingly, this set up also created an air liquid interface.

Due to the reduced diffusion pathways for the blocking set up, slower dissolution profiles were expected than for those without blocking. This could not be shown for Budesonide (Fig. 4). Most of the dissolved amount of substance diffuses through the membrane and not over the edge the between membrane and membrane holder. For Substance A dibromide and Substance A amorphous base, the diffusion process in the blocking set up is much slower (Fig. 5b compared to Fig. 5c). Substance A dibromide (c_s = 265 µg/ml) and Substance A amorphous base (c_s = 211 µg/ml) both have a solubility more than 10 times higher than Budesonide (c_s = 17 µg/ml) (7), so the diffusion rate is the limiting step and not the solubility. By preventing diffusion over the membrane rim, diffusion is only possible through the membrane.

The idea behind the membrane sandwich holder was to reduce possible effects of the watch glass on the diffusion and therefore on the dissolution process. There are two different zones above and below the membrane holder. Above, there is a low concentration of diffused substance because of the constant movement of the paddle. Consequently, the diffusion gradient is high and the dissolved substance moves faster through the upper membrane. Beneath the watch glass, the dissolution medium is almost unstirred and convection is relatively slow (11). The concentration of dissolved substance directly at the lower membrane is very high, but due to the low convection, the diffusion gradient is small and substance tends to pass through the upper side of the membrane at. Therefore, changing the watch glass to a mesh does not influence the dissolution process (Fig. 4, f_1 = 5.8, f_2 = 65.3).

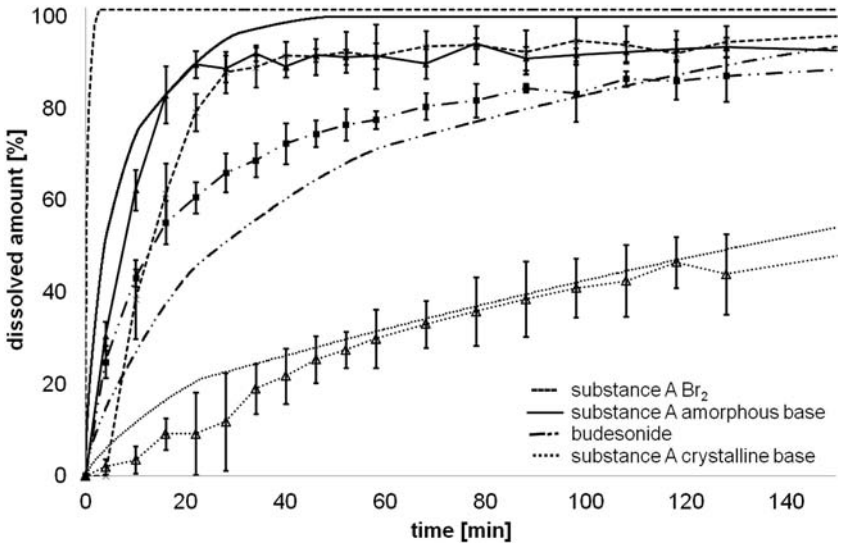

Fig. 9 Comparison of model data (*no symbols*) with experimental data (*symbols*) of the tested substances (Substance A dibromide - - -; Substance A amorphous base —, Budesonide – · ·, Substance A crystalline base ···); set up: mACI and 0.02% DPPC in PBS buffer, mean ± SD, $n = 3$.

Overall the "standard" membrane holder adapted from the transdermal patches is advantageous in comparison to the other membrane holders tested (blocked and sandwich). With the membrane holders used in this study, the substance particles are placed directly on the membrane and the diffused dissolution medium has direct access to the particles for dissolving. Possible air bubbles between the watch glass and membrane have no impact on the dissolution process.

Furthermore, it could be supposed that the "standard" membrane holder used yields better results than the system described by Son *et al.* They used the next generation impactor, in which a membrane is placed on top of the deposited powder in the sample pan, sealing the cassette (11). This traps air under the membrane, which could slow down or even hinder the access of dissolution medium to the API particles, resulting in reduced dissolution (37).

In this study surfactants are used to increase the discriminating power between the different substances. In Table I the solubility data of substances in PBS buffer with and without surfactants are compared to each other. Surfactants are also used to increase the wettability of the substances, but not the solubility. If the solubility is increased, the discrimination power between the different substances is reduced. It is obvious that SDS and Tween® 20 strongly increase the solubility of Budesonide and Substance A base. Hence, these two surfactants are not suitable for our tests and DPPC was chosen instead. The objects size of DPPC are too large to pass through the filter (Table I, (11)). However, the micelles act as a reservoir for DPPC molecules (31), and the free DPPC molecules are able to pass through the membrane and can improve the wettability of substances, resulting in a better reproducibility of the dissolution process.

In contrast to our earlier publication were in which we were able to discriminate between Substance A amorphous base, Substance A Br_2 and Budesonide (7), we did not observe different dissolution profiles by varying the major influencing factors, especially particle mass and distribution on the membrane. Although the model data supports this effect, it is calculated under the assumptions described above. With optimized deposition (mass and distribution), it can be seen that the set up is no longer able to distinguish between he substances which is again in line with the theoretical data. By adding 0.02% DPPC to the dissolution medium, discrimination between the substances used (Fig. 5b) is possible in the experimental as well as in the model approach.

In the second part of the study we describe a model for modeling the dissolution profile of powders for inhalation and other influencing factors under investigation. We showed that solubility, diffusion layer thickness, particle shape, and particle size distribution, especially for particles between 10 and 1.5 μm strongly influences the dissolution profiles.

For particles with a diameter of less than 30 μm it is postulated that diffusions layer thickness is dependent on radius (24,26,30). Our calculations support this hypothesis. Furthermore, we showed that a time dependent diffusion layer (28) can be assumed. Models with an individual time independent diffusion layer thickness for each particle size class or rather underestimates the experimental dissolution profiles. However, if the value chosen for h is too small, the model strongly overestimates the experimental data.

The model also demonstrates the influence of particle size on the dissolution profile. As expected, decreasing particle size increases the speed of the dissolution profile due to increased particle surface. From the comparison of these modeled data and the experimental data for the different dose collection methods, it can be assumed that by using mACI, the particles on the membrane are less agglomerated compared to the aACI set up.

Furthermore, the model demonstrates the high impact of solubility on the dissolution profile, *e.g.*, by adding surfactants.

A comparison of experimental data and the models (Fig. 9) for Budesonide and Substance A amorphous base shows that they are in agreement. The model for Substance A Br_2 overestimates the experimental data. This is because of the high solubility for Substance A Br_2 with 0.02% DPPC in the dissolution media. If the solubility data in the model is converted to the solubility of the Br_2 in PBS buffer, the model and experimental data converge.

Conclusion

In this study we described a new dose collection method that ensures a more homogeneous particle distribution on the membrane, and thus minimizes the influence of the deposited mass on the observed dissolution profiles. The addition of 0.02% DPPC improves the wettability of substances, resulting in better discrimination of dissolution profiles and good reproducibility as confirmed by the fit factor test. Furthermore, we were able to show that with a theoretical model based on the Nernst-Brunner equation, it is possible to predict the dissolution profiles of powders for inhalation.

ACKNOWLEDGMENTS AND DISCLOSURES

Thanks to Dr. Holger Wagner, Dr. Peter Häbel and team (Boehringer Ingelheim) for calculating the van der Waals volumes of the substances and to Wolfgang Bootz (Boehringer Ingelheim) and Dr. Bernhard Meier for the SEM pictures.

REFERENCES

1. Gray VA, Hickey AJ, Balmer P, Davies NM, Dunbar C, Foster TS, *et al.* The inhalation ad hoc advisory panel for the USP performance tests of inhalation dosage forms. Pharmacopeial Forum. 2008;34:1068–74.
2. United States Pharmacopeial Convention. Dissolution. In United States Pharamacopeia and National Formulary, Rockville, 2011.
3. United States Pharmacopeial Convention. Drug release. In United States Pharmacopeia and National Formulary, Rockville, 2013.
4. United States Pharmacopeial Convention. Aerosol, nasal sprays, metered dose inhalers, and dry powder inhaler. In United States Pharmacopeia and National Formulary, Maryland, 2012.
5. Labouta HI, Schneider M. Tailor-made biofunctionalized nanoparticles using layer-by-layer technology. Int J Pharm. 2010;395:236–42.
6. Riley T, Christopher D, Arp J, Casazza A, Colombani A, Cooper A, *et al.* Challenges with developing in vitro dissolution tests for orally inhaled products (OIPs). AAPS PharmSciTech. 2012;13:978–89.
7. May S, Jensen B, Wolkenhauer M, Schneider M, Lehr CM. Dissolution techniques for in vitro testing of dry powders for inhalation. Pharm Res. 2012;29:2157–66.
8. Salama RO, Traini D, Chan HK, Young PM. Preparation and characterisation of controlled release co-spray dried drug-polymer microparticles for inhalation 2: evaluation of in vitro release profiling methodologies for controlled release respiratory aerosols. Eur J Pharm Biopharm. 2008;70:145–52.
9. Haghi M, Traini D, Bebawy M, Young PM. Deposition, diffusion and transport mechanism of dry powder microparticulate salbutamol, at the respiratory epithelia. Mol Pharm. 2012;9:1717–26.
10. Arora D, Shah KA, Halquist MS, Sakagami M. In vitro aqueous fluid-capacity-limited dissolution testing of respirable aerosol drug particles generated from inhaler products. Pharm Res. 2010;27:786–95.
11. Son YJ, Horng M, Copley M, McConville JT. Optimization of an in vitro dissolution test method for inhalation formulations. Dissolution Technol. 2010;17:6–13.
12. Davies NM, Feddah MR. A novel method for assessing dissolution of aerosol inhaler products. Int J Pharm. 2003;255:175–87.
13. Sakagami M, Arora Lakhani D. Understanding dissolution in the presence of competing cellular uptake and absorption in the airways. In: Dalby RN, Byron PR, Peart J, Suman JD, Farr SJ, Young PM, editors. Respiratory Drug Delivery. 2012, pp. 185–192.
14. Mees J, Fulton C, Wilson S, Bramwell N, Lucius M, Cooper A. Development of dissolution methodology for dry powder inhalation aerosols. IPAC-RS Conference In 2011.
15. Veldhuizen R, Nag K, Orgeig S, Possmayer F. The role of lipids in pulmonary surfactant. Biochim Biophys Acta Mol basis Dis. 1998;1408:90–108.
16. Dokoumetzidis A, Macheras P. A century of dissolution research: from Noyes and Whitney to the Biopharmaceutics classification system. Int J Pharm. 2006;321:1–11.
17. Hsu W-L, Lin M-J, Hsu J-P. Dissolution of solid particle in liquids: a shrinking core model. World Acad Sci Eng Technol. 2009;53:913–8.
18. Wang J, Flanagan DR. General solution for diffusion-controlled dissolution of spherical particles. 1. Theory. J Pharm Sci. 1999;88:731–8.
19. Son YJ, McConville JT. Development of a standardized dissolution test method for inhaled pharmaceutical formulations. Int J Pharm. 2009;382:15–22.
20. Jensen B, Reiners M, Wolkenhauer M, Ritzheim P, May S, Schneider M, et al. Dissolution testing for inhaled products. Respiratory Drug Delivery, Europe In 2011, pp. 303–308.
21. May S, Jensen B, Wolkenhauer M, Schneider M, Lehr CM. Impact of deposition and the presence of surfactants on in vitro dissolution of inhalation powders. Respiratory Drug Delivery Europe In 2013.
22. Food and Drug Administration. Guidance for Industry; Dissolution testing of immediate release solid oral dosage forms. http://www.fda.gov/downloads/Drugs/GuidanceComplianceRegulatoryInformation/Guidances/ucm070237.pdf online (1997).
23. European Medicines Agency. Guideline on the investigation of bioequivalence. http://www.ema.europa.eu/docs/en_GB/document_library/Scientific_guideline/2010/01/WC500070039.pdf online (2008).
24. Sertsou G. Analytical derivation of time required for dissolution of monodisperse drug particles. J Pharm Sci. 2004;93:1941–4.
25. Hayduk W, Laudie H. Prediction of diffusion coefficients for nonelectrolytes in dilute aqueous solutions. AIChe. 1974;20:611–5.
26. Sheng JJ, Sirois PJ, Dressman JB, Amidon GL. Particle diffusional layer thickness in a USP dissolution apparatus II: a combined function of particle size and paddle speed. J Pharm Sci. 2008;97:4815–29.
27. Bisrat M, Nystrom C. Physicochemical aspects of drug release. VIII. The relation between particle size and surface specific dissolution rate in agitated suspensions. Int J Pharm. 1988;47:223–31.
28. Lu ATK, Frisella ME, Johnson KC. Dissolution modeling: factors affecting the dissolution rates of polydisperse powders. Pharm Res. 1993;10:1308–14.
29. Hintz RJ, Johnson KC. The effect of particle size distribution on dissolution rate and oral absorption. Int J Pharm. 1989;51:9–17.
30. Sugano K. Theoretical comparison of hydrodynamic diffusion layer models used for dissolution simulation in drug discovery and development. Int J Pharm. 2008;363:73–7.

31. Voigt R. Pharmazeutische Technologie. Stuttgart: Deutscher Apotheker Verlag; 2006.
32. Nichols SC. Calibration and mensuration issues for the standard and modified andersen cascade impactor. Pharmacopeial Forum. 2000;26:1466–7.
33. Okazaki A, Mano T, Sugano K. Theoretical dissolution model of poly-disperse drug particles in biorelevant media. J Pharm Sci. 2008;97:1843–52.
34. Davies CN. Particle-fluid interaction. J Aerosol Sci. 1979;10:477–513.
35. http://www.guidechem.com/dictionary/de/51333-22-3.html. 2013.
36. Sadler RC, Prime D, Burnell PK, Martin GP, Forbes B. Integrated in vitro experimental modelling of inhaled drug delivery: deposition, dissolution and absorption. J Drug Deliv Sci Technol. 2011;21:331–8.
37. Wauthoz N, Deleuze P, Saumet A, Duret C, Kiss R, Amighi K. Temozolomide-based dry powder formulations for lung tumor-related inhalation treatment. Pharm Res. 2011;28:762–75.